Radiotherapy and Oncology 141 (2019) 208–213

Contents lists available at ScienceDirect

Radiotherapy and Oncology

journal homepage: www.thegreenjournal.com

Original Article

Validation of different PSMA-PET/CT-based contouring techniques for intraprostatic tumor definition using histopathology as standard of reference

Constantinos Zamboglou [a,l,m,1], Thomas F. Fassbender [b,*,1], Lina Steffan [a,l], Florian Schiller [b], Tobias Fechter [c], Montserrat Carles [c], Selina Kiefer [d,l], Hans C. Rischke [a,l], Kathrin Reichel [e], Nina-Sophie Schmidt-Hegemann [f], Harun Ilhan [g], Alin F. Chirindel [h], Guillaume Nicolas [h], Christoph Henkenberens [i], Thorsten Derlin [j], Peter Bronsert [d,l], Panayiotis Mavroidis [k], Ronald C. Chen [k], Philipp T. Meyer [b], Juri Ruf [b,1], Anca L. Grosu [a,l,1]

[a] Department of Radiation Oncology; [b] Department of Nuclear Medicine; [c] Division of Medical Physics, Department of Radiation Oncology; [d] Department of Pathology; [e] Department of Urology, Medical Center – University of Freiburg, Faculty of Medicine. University of Freiburg; [f] Department of Radiation Oncology; [g] Department of Nuclear Medicine, University Hospital, LMU Munich; [h] Department of Radiology and Nuclear Medicine, University Hospital Basel; [i] Department of Radiation Oncology; [j] Department of Nuclear Medicine, Hannover Medical School, Germany; [k] Department of Radiation Oncology, University North Carolina – Chapel Hill, USA; [l] German Cancer Consortium (DKTK), Partner Site Freiburg; and [m] Berta-Ottenstein-Programme, Faculty of Medicine, University of Freiburg, Germany

ARTICLE INFO

Article history:
Received 23 May 2019
Received in revised form 28 June 2019
Accepted 2 July 2019
Available online 17 August 2019

Keywords:
PSMA-PET/CT
Primary prostate cancer
Delineation
Contouring
Histopathology

ABSTRACT

Purpose: Accurate definition of the intraprostatic gross tumor volume (GTV) is crucial for diagnostic and therapeutic approaches in patients with primary prostate cancer (PCa). The optimal methodology for contouring of GTV using Prostate specific membrane antigen positron emission tomography (PSMA-PET) information has not yet been defined.

Methods and Materials: PCa patients who underwent a [68Ga]PSMA-11-PET/CT followed by radical prostatectomy were prospectively enrolled ($n = 20$). Six observer teams with different levels of experience and using different PET image scaling techniques performed manual contouring of GTV. Additionally, semi-automatic segmentation of GTVs was performed using SUVmax thresholds of 20–50%. Coregistered histopathological gross tumor volume (GTV-Histo) served as reference. Interobserver agreement was assessed by calculating the Dice similarity coefficient (DSC).

Results: Most contouring methods provided high sensitivity and specificity. For manual delineation, scaling the PET images from SUVmin-max: 0–5 resulted in high sensitivity (>86%). The highest specificity (100%) was obtained by scaling the PET images from SUVmin-max: 0-SUVmax. High interobserver agreement (median DSC 0.8) was observed when using the same PET image scaling technique (PET images SUVmin-max: 0–5). For semi-automatic segmentation, a low SUVmax threshold of 20% optimized sensitivity (SUVmax threshold 20%, 100% sensitivity, 32% of prostatic volume), whereas a higher threshold optimized specificity (SUVmax threshold 40%–50%, 100% specificity).

Conclusions: Contouring of regions with high tracer-uptake resulted in very high specificities and should be used for biopsy guidance. Both manual and semi-automatic approaches using validated SUV scaling (SUVmin-max: 0–5) or thresholding (20%) may provide high sensitivity, and should be considered for PSMA-PET-based focal therapy approaches.

© 2019 Elsevier B.V. All rights reserved. Radiotherapy and Oncology 141 (2019) 208–213

The identification and accurate contouring of the intraprostatic tumor volume is a crucial step for diagnostic and therapeutic approaches in patients with primary prostate cancer (PCa). In the last decade the concept of focal radiation therapy (RT) has gained interest for patients with PCa and boosting the RT dose to the visible tumor areas within the prostate may improve treatment outcome [1,2]. Moreover, recurrent PCa after conventional RT often occurs at the site of the primary tumor [3,4]. Currently, several phase III trials (e.g. the FLAME trial [5]) are investigating the treatment outcomes after focal RT dose escalation for patients with primary PCa.

* Corresponding author at: Department of Nuclear Medicine, Medical Center – University of Freiburg, Hugstetter Str. 55, D-79106 Freiburg Germany.
E-mail address: thomas.fassbender@uniklinik-freiburg.de (T.F. Fassbender).
[1] Authors contributed equally.

https://doi.org/10.1016/j.radonc.2019.07.002
0167-8140/© 2019 Elsevier B.V. All rights reserved.

Most of the studies investigating targeted biopsies or focal therapy regimen in patients with PCa used MRI information for intraprostatic tumor delineation [6]. However, MR image interpretation for PCa diagnosis results in substantial inter-reader variability [7] which impacts intraprostatic tumor delineation [8,9].

Radioactive-labeled tracers targeting the prostate specific membrane antigen (PSMA) have been implemented for positron emission tomography (PET) in patients with primary PCa. Previous work by our group [10,11], which is in agreement with the findings of other studies [12,13] has suggested that PSMA-PET may be superior to MRI for intraprostatic tumor detection and focal therapy guidance. In the latter studies the detection and delineation of intraprostatic PCa was mainly performed manually by experienced readers.

However, a consensual and largely accepted method to accurately delineate the intraprostatic tumor volume based on PSMA-PET information has not yet been established. In this context, we have enrolled 20 patients with PCa and a PSMA-PET/CT before surgery in a prospective study design, for who PET-based prostate tumor delineation was performed by different semi-automatic segmentation methods as well as by manually defined contours from different observers. The distribution of PCa in coregistered histopathologic information served as the standard of reference.

Methods and materials

Patients

Between February 2014 and July 2018, 20 patients with histopathologically proven primary PCa, pre-therapeutic [68Ga]-PSMA-11-PET/CT scan and intended radical prostatectomy were prospectively enrolled. Exclusion criteria were ongoing androgen deprivation therapy, >3 months' time gap between PSMA-PET/CT scan and operation and previously performed transurethral resection of the prostate. Written informed consent was obtained from all patients, and the institutional review board approved this study. Please see supplementary Table 1 for detailed patients' characteristics.

PET/CT imaging

A detailed description of our radiolabelling protocol of [68Ga]-PSMA-11 can be found in Zamboglou et al. [14]. One hour after intravenous tracer injection, patients underwent whole body PET scan after voiding. Whole body acquisition protocols were acquired on three different Philips scanners: GEMINI TF TOF 64, GEMINI TF 16 Big Bore and Vereos. All scanners fulfilled the requirements indicated in the European Association of Nuclear Medicine (EANM) imaging guidelines and obtained EANM Research Ltd. (EARL) accreditation during acquisition [15,16]. All systems resulted in a PET image with a voxel size of $2 \times 2 \times 2$ mm^3. Images were normalized to decay corrected injected activity per kg body weight (standardized uptake values, SUV in [g/ml]). As a result of the EARL accreditation process, comparable SUV parameters were derived from these 3 scanners. However, we additionally performed an extended evaluation of SUV comparability by phantom studies as described in supplementary material 1.

Histopathology and PET/CT image coregistration

The 3D distribution of PCa in the prostatectomy specimen served as ground truth and was obtained using a published, in-house coregistration protocol [11,17]. After formalin fixation, the resected prostate specimen underwent an ex-vivo CT scan using a customized localizer. To ensure equal cutting angels between the tissue specimens and ex-vivo CT slices, whole-mount step sections were cut every 4 mm using an in-house cutting device. All tissue specimens were paraffin embedded and sliced using a Leica microtom. Staining with hematoxylin and eosin was performed via routine protocols and PCa tissue was delineated by two pathologists. Histology slices were registered on ex-vivo CT images and PCa contours were transferred onto the CT images. The contours were interpolated by 2 mm expansion in both Z-axis directions to create a model of the 3D distribution of PCa in histology (GTV-Histo). Taking into account the non-linear transformations of the prostatic gland after resection, ex-vivo CT (including GTV-Histo contours) was registered on in-vivo CT (from PSMA-PET/CT scans) by manual coregistration allowing elastic deformations. The final alignment of in-vivo CT and PET scans was based on the hardware coregistration of the hybrid PET/CT scanners. In 20% of the patients a misalignment between PET and CT images occurred (up to 2 cm) and a manual adaption was applied using rigid registration. For better orientation, the prostatic gland was delineated on CT and PET images.

Table 1
Observer teams.

Team	Level of experience in PSMA PET interpretation	Scaling technique	Software used for segmentation
Team1	high	SUVmin-max: 0–5*	iPlan v4.7.7
Team2	high	Adjustment of gray scale PET images using window center and width	OncentraMasterplan
Team3	high	SUVmin-max: 0–7.5	OncentraMasterplan
Team4	high	SUVmin-max: 0-SUVmax	MIM software
Team5	high	SUVmin-max: 0–5*	iPlan v4.7.7
Team6	no experience	SUVmin-max: 0–5*	iPlan v4.7.7

High level of experience was defined as: (i) >2 years of experience in PSMA PET-image interpretation and (ii) all readers were board-licensed nuclear medicine physicians or radiation oncologists.

* Teams 1, 5 and 6 set the maximum and minimum voxel values from 0 to 5 SUV when displaying PET images for contouring. Presence of PCa on PET images was defined as mono- or multifocal uptake greater than adjacent background in more than one slice within the CT-defined prostate gland.

Delineations based on PET images

Contouring of intraprostatic gross tumor volume (GTV) was performed in PSMA-PET images for all 20 patients using three different approaches (Fig. 1):

Manual delineations: four teams of delineators were recruited from four different university medical centers (GTV-Team1–4). Each team consisted of two board-licensed readers with >2 years of experience in interpretation of PSMA-PET images. On PSMA-PET images the intraprostatic tumor mass was delineated according to local practice. The accompanying CT scans were provided for anatomical orientation. To ensure that the study results were representative for a realistic clinical situation, the teams used the delineation system of their own hospital (Table 1). Apart from PET/CT images no further clinical information of the patients was provided. A first interim-analysis revealed that team 1 achieved the highest sensitivity of all four teams. Subsequently, one team with two experienced readers (GTV-Team5) and one team consisting of two readers with no experience in PSMA-PET image interpretation (GTV-Team6) also delineated the PSMA-PET images of all patients using the same scaling technique as team 1.

Threshold segmentations: By applying a threshold of 20%, 30%, 40% and 50% of intraprostatic SUVmax, respectively, GTV-20%–50% were segmented semi-automatically in iPLan v4.1.1. (Brainlab).

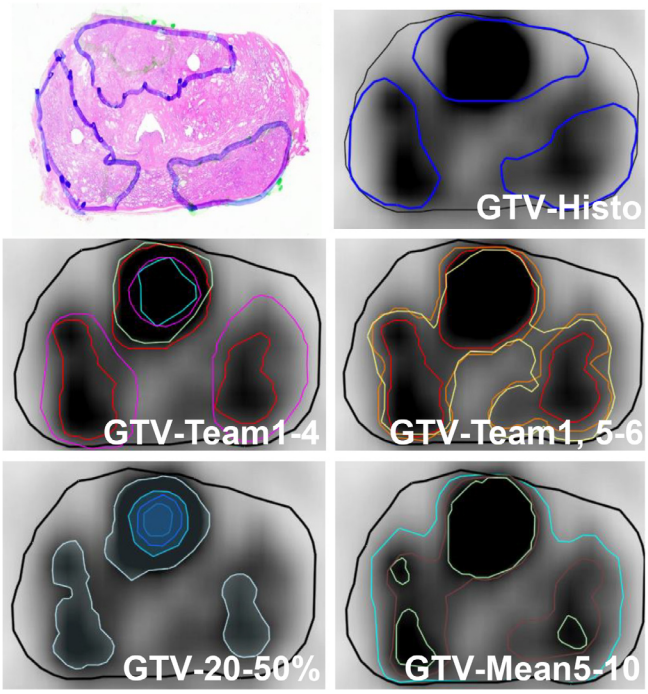

Fig. 1. Image segmentations. In the left upper row H&E stained whole-mount surgery specimen is shown with PCa marked in blue. In the other images an axial PSMA-PET image is shown including the respective GTVs. PET image scaling is SUVmin-max: 0–5. Manual GTV-Delineations by team are color-coded as follows: red = GTV-Team1, purple = GTV-Team2, blue = GTV-Team3, green = GTV-Team4, yellow = GTV-Team5, orange = GTV-Team6. The prostatic contour is marked in black.

Tumor/normal tissue ratio segmentations: Another approach to define a threshold for semi-automatic segmentation on PET images is to define a ratio between tumor tissue and a background signal [18,19]. To obtain the background signal in our study, two spherical volumes of interest (VOIs) with 1 cm diameter were placed in the left and right gluteus maximus muscle of each patient, respectively, and the mean SUV value of all 4 VOIs were calculated (median value for all patients: 0.38, range: 0.28–0.71). The median ratio between the SUVmean and SUVmin values in GTV-Histo and the background signal were approximately 10 and 5, respectively. Likewise, we multiplied each patient's background signal by 5, 7.5 and by 10, respectively, to obtain a threshold for semi-automatic creation of GTV-Mean5, GTV-Mean7.5 and GTV-Mean10 in iPLan v4.1.1. (Brainlab).

Finally, all PET scans including the all contours were imported into Eclipse v15.1 (Varian) and registered using hardware-based coregistration. The corresponding CT scan was also registered by hardware-based coregistration and all contours were transferred from the PET images to the corresponding CT scan. The contour of the prostatic gland on CT images was delineated by an experienced radiation oncologist.

Statistical analysis

The statistical analysis was performed on GraphPad Prism v7.04 (GraphPad Software). To compare two different groups the Wilcoxon matched-pairs signed rank test for pairwise testing was used. This was due to the fact that the variables were not normally distributed. The two-stage step-up method of Benjamini, Krieger and Yekutieli [20] was used to correct for multiple comparisons by controlling the false discovery rate with a significance level at 0.05. The overlap between the different GTVs as well as their proportion to the prostatic gland was measured in the Eclipse planning software. We assessed the agreement between different manual contours at voxel level using the Dice similarity coefficient (DSC) [21]. When applied at voxel level, this index is identical to the kappa index [8]. Additionally, we calculated the sensitivities and specificities for all GTVs based on the histology standard of reference data by dividing the prostate in each CT slice into 4 equal segments as performed previously by our group [11]. Finally, Spearman correlation coefficients (ρ) were calculated to assess whether the reached sensitivities and GTV-Histo coverage of the different delineation methods correlate with clinical surrogate parameters (GTV-Histo volume, PSA serum level before PET imaging, Gleason score in surgery specimen).

Results

For teams 1–4 a great heterogeneity regarding the PET scaling technique was observed (Table 1) and a moderate interobserver agreement was calculated: median DSC 0.56 (range: 0–0.94). Teams 1, 5 and 6 applied the same PET scaling technique (SUVmin-max: 0–5) and the interobserver agreement was very high 0.8 (range: 0.3–0.96). GTV-Team3 and 4 ($p < 0.01$) but not GTV-Team2 ($p > 0.05$) were statistically significant smaller than GTV-Histo. The contours of team 1, 5 and 6 had no statistically significant differences to the volume of GTV-Histo ($p > 0.05$), respectively. They covered at least 60% of GTV-Histo and had median sensitivities of ≥86% (Table 2 and Fig. 2A). We observed low to moderate correlations between clinical surrogate parameters and the reached sensitivities and GTV-Histo coverage of teams 1, 5 and 6 (supplementary Table 2). All 6 teams reached a high median specificity (>73%) and two manual contours (team 3 and 4) had median specificities of 100%, respectively. A median proportion of 17–25% of the prostatic gland was encompassed by the GTVs of team 1, 5 and 6 and GTV-Team3 encompassed only 1% of the prostatic gland volume.

In the next step, reader independent segmentation approaches were evaluated. As expected, the approaches applying the lowest SUV thresholds (GTV-20% and GTV-Mean5) covered the highest amount of GTV-Histo: both with median coverage of >80% and sensitivities of 100%, respectively. Compared to the manual contours of team 1, 5 and 6, GTV-Mean5 but not GTV-20% had a statistically significant higher coverage of GTV-Histo (Fig. 2B). Low to moderate correlations between clinical surrogate parameters and the reached sensitivities and GTV-Histo coverage of GTV-20% and GTV-Mean5 were observed (please see supplementary Table 2). Two SUVmax-based segmentations (40% and 50%) had a median specificity of 100%, respectively. A median proportion of 32% and 68% of the prostatic gland were encompassed by GTV-20% and GTV-Mean5, respectively.

Please see Table 2 for a detailed listing of the GTV volumes, their proportion to the prostatic gland total volume as well as their sensitivities and specificities.

Discussion

The use of PSMA-PET imaging has increased in the last years and a few studies suggest an excellent performance of PSMA-PET for intraprostatic tumor detection [22]. So far, on a voxel-wise correlation between PSMA-PET and histology, a threshold of 30% of SUVmax within the prostate was proposed for semi-automatic PCa segmentation [17]. Two other studies used different thresholds for PSMA-based intraprostatic tumor segmentation: 40% and 50% of SUVmax within the prostate, respectively [23,24]. However, a consensus on how to accurately delineate the intraprostatic tumor volume based on PSMA-PET information has not yet been reached.

Table 2
Overview of PSMA PET based segmentations techniques in comparison with histology reference.

	Median volume in ml (25–75% percentile)	Median proportion of prostatic volume in % (25–75% percentile)	Median sensitivity in % (25–75% percentile)	Median specificity in % (25–75% percentile)
GTV-Histo	9.7 (2.8–19.8)	17 (6–30)		
GTV-Team1	10 (3–24)	18 (5–47)	86 (78–97)	92 (72–100)
GTV-Team2	9.3 (3–21.7)	16 (8–33)	75 (58–97)	98 (83–100)
GTV-Team3	1 (0.4–2.2)	1 (1–6)	32 (11–70)	100 (91–100)
GTV-Team4	6.6 (1.7–23.3)	12 (2–40)	83 (41–100)	100 (85–100)
GTV-Team5	11.1 (5.3–29)	25 (9–55)	89 (85–100)	73 (50–97)
GTV-Team6	10.3 (4.3–28)	23 (7–54)	88 (77–97)	80 (41–92)
GTV-20%	17.5 (12.5–37.2)	32 (18–67)	100 (89–100)	67 (11–100)
GTV-30%	8 (3.1–19.9)	14 (7–44)	83 (64–100)	90 (67–100)
GTV-40%	3.9 (1.5–10.5)	5 (4–18)	74 (39–88)	100 (80–100)
GTV-50%	1.4 (0.8–3.7)	2 (1–6)	50 (27–76)	100 (90–100)
GTV-Mean5	29.7 (21.5–40.2)	58 (40–70)	100 (96–100)	43 (25–100)
GTV-Mean7.5	12.4 (4.5–31.6)	26 (7–50)	86 (65–98)	85 (58–100)
GTV-Mean10	7.9 (1–19.3)	12 (2–23)	82 (59–93)	94 (76–100)
Prostate	57 (42.5–79.1)			

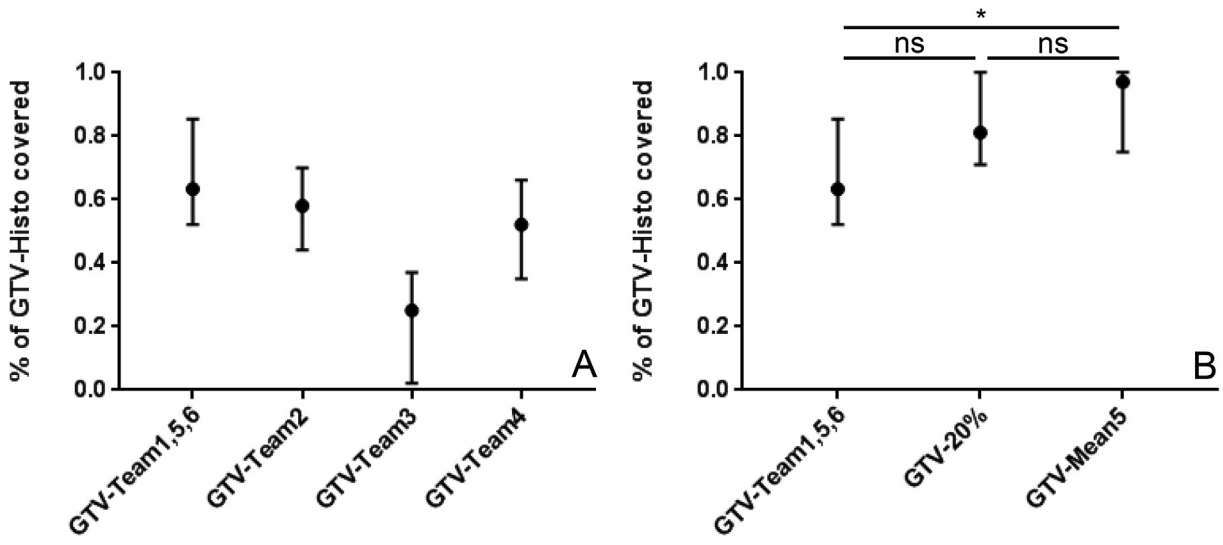

Fig. 2. Coverage of GTV-Histo. The median and the interquartile ranges for GTVs over all patients are shown. The mean overlap with GTV-Histo for GTVs of teams 1, 5 and 6 over all patients is named GTV-Team1, 5, 6. In (A) GTV-Histo coverage by manually created GTVs is presented. Friedman test showed statistically significant differences in overlap with GTV-Histo between all teams ($p < 0.01$). In (B) GTV-Team1, 5, 6 was compared with the best performing semi-automatic segmentations (GTV-20% and GTV-Mean5). GTV-Mean5 covered a statistically significantly higher amount of GTV-Histo compared to manually delineated GTVs ($p < 0.05$) but not compared to GTV-20% ($p = 0.135$). The coverage of GTV-Histo by GTV-20% was not statistically significantly higher ($p > 0.05$) compared to manually segmented GTVs using SUVmin-max: 0–5 for PET image scaling. Abbreviations: n.s. = not statistically significantly, * = $p < 0.05$.

Not surprisingly, this study showed a great variability in different manual and semi-automatic contouring approaches for the intraprostatic tumor volume based on PSMA-PET information. In comparison with histology as the reference, we tried to identify contouring approaches which offered an excellent performance for focal therapy guidance (high sensitivity) as well as for targeted biopsy approaches (high specificity). In the following, we discuss our results in detail.

A moderate agreement was observed (DSC 0.56) between PCa contours of teams 1–4. Underlying delineation differences can be explained by different PET image scaling techniques employed, since all teams had high-level of experience but used different scaling levels for PET images during contouring. However, interobserver variance is also a known issue for other imaging modalities such as MRI. In a study by Steenbergen et al. interobserver agreement in MRI-based PCa contouring was analyzed and compared with histology reference. The interobserver agreement between the contours of 6 teams and the histology reference was moderate (kappa 0.45) and one PCa lesion in the central zone was missed by all teams [8]. Rischke et al. was able to prove that a diffusion-weighted (DWI)-MRI (kappa 0.51) based tumor delineation resulted in lower intraobserver agreement compared to perfusion (DWE)- or T2w-based approaches (kappa > 0.61) [25]. In the current study, a very high interobserver agreement (DSC = 0.8) was calculated for 3 teams that, despite different experience, used the same windowing level (SUVmin-max: 0–5), indicating that even readers with different experience levels achieve comparable results in GTV contouring when the same PET image scaling technique is used.

A high specificity is required for targeted biopsies in patients with primary PCa in order to increase the chance to detect PCa in biopsy tissue. It is not surprising that the contouring techniques which covered mainly the regions with highest tracer uptake reached the highest specificities. Two teams (3 and 4) used a maximum SUV > 5 for scaling during delineation and reached median specificities of 100%. In line with this observation, two of the SUVmax-related segmentations (threshold of 40% and 50% of SUVmax) had also a specificity of 100%. It should be mentioned that the GTVs with high specificities were statistically significantly smaller than GTV-Histo and as a result a high amount of intraparostatic

PCa was not covered by them. However, a recent work from Bravacini and colleagues demonstrated that the PSMA expression in PCa lesions correlates with Gleason score [26]. Thus, it is very likely that the regions with highest tracer uptake also represent the regions with the highest Gleason score.

Obviously, RT dose escalation to large target volumes including a lot of normal tissue (low specificity) increases toxicity. On the other hand, boosting too small volumes (low sensitivity) may reduce tumor control. It should be mentioned that PCa possesses intratumoral heterogeneity [27] and it is not clear whether the regions with the highest tracer uptake also encompass the clinical relevant part of the disease, e.g. the radio resistant cells. Until this issue is answered, most likely, the tumor control after focal RT approaches depends on the amount of coverage of the entire intraprostatic tumor mass. Thus, a high sensitivity is demanded for PSMA-guided focal therapy approaches. One manual (PET image scaling SUVmin-max: 0–5) and one semi-automatic (20% of SUVmax) contouring technique reached comparable results by covering $\geq$60% of GTV-Histo with sensitivities of $\geq$86%. GTV-Mean5 covered a significantly higher amount of GTV-Histo than manual contours but not more than GTV-20%. It should be mentioned that the median volume of GTV-Mean5 was statistically significantly larger than the other volumes by encompassing 58% of the prostatic gland. The median volumes of GTV-20% and GTV-Team1, 5 and 6 comprised 32% and 18–25% of the prostate volume ($p > 0.05$), respectively. Consequently, both approaches should firstly be considered for PSMA-based focal therapy approaches. Future studies should investigate whether the differences in coverage of GTV-Histo or in the proportion to the prostatic gland can be translated in better tumor control or in increased normal tissue toxicity after focal RT, respectively. It should be mentioned that the depiction of PCa lesions in PSMA-PET imaging depends on tumor volume, tumor shape and its biology. Thus, it is unlikely that one segmentation technique performs best for all PCa lesions. Additionally, in some patients even the GTVs with the highest sensitivity covered less than 50% of GTV-histo. This observation may be explained by a work of Mannweiler et al. which reported that 6 of 51 examined intraprostatic lesions had no or low PSMA expression [28]. In this work, we analyzed whether clinical surrogate parameters influence the performance of PSMA-based delineations in terms of sensitivity and GTV-histo coverage. Since only low to moderate correlations were found, an accurate surrogate parameter-based prediction of the tumor coverage by PSMA PET contours is not possible. Consequently, we suggest maintaining a sufficient RT dose to the whole prostate in order to prevent under treatment of undetected PCa in focal RT for intermediate and high-risk PCa patients. In addition, two recent studies postulated that MR imaging may offer complementary information to PSMA-PET [12,14]. Future studies should address whether the combined usage of MR and PSMA-PET may further increase PCa detection and allow RT dose de-escalation to the rest of the prostatic gland.

A potential limitation of our study is the uncertainty in correlation of PET/CT and histopathology (e.g. non-linear shrinkage of the prostate after prostatectomy). Thus, it could not be excluded that moderate or low coverage of GTV-histo by the PET-derived GTVs is a consequence of mismatch in coregistration or incomplete histopathological coverage instead of poor tracer or reader performance. However, as the calculation of sensitivities and specificities was not performed on a voxel-level but on a less stringent slice by slice level, we consider the potential resulting bias negligible. A second issue of our study is that different PET/CT scanners were used. However, all scanners fulfilled the EARL accreditation prerequisites and phantom studies confirmed the comparability of SUV values between the three scanning systems. Third, due to the elaborate pathology-imaging co-registration protocol, the sample size in our study is relatively small. Fourth, we caused a selection bias by only enrolling patients scheduled for prostatectomy in order to obtain histopathologic information from surgical specimen. As a result, the findings from our study are strictly speaking only representative for intermediate- and high-risk PCa patients. Further studies need to proof our results for low-risk PCa patients.

In conclusion, our study identified manual and semi-automatic contouring approaches for PSMA-PET-based intraprostatic GTV delineation using co-registered histology as standard of reference. For targeted biopsy guidance a high specificity is demanded and delineation of regions with high tracer-uptake can be applied. To obtain a high sensitivity for PSMA-PET-based focal RT approaches manual delineation with PET image scaling of SUVmin-max: 0–5 or a semi-automatic approach by applying a threshold of 20% of SUVmax are recommended.

Declaration of Competing Interest

None.

This study was not funded by any third party organization.

Responsible for statistical analyses were Constantinos Zamboglou and Tobias Fechter.

Appendix A. Supplementary data

Supplementary data to this article can be found online at https://doi.org/10.1016/j.radonc.2019.07.002.

References

[1] Zamboglou C, Sachpazidis I, Koubar K, Drendel V, Wiehle R, Kirste S, et al. Evaluation of intensity modulated radiation therapy dose painting for localized prostate cancer using 68Ga-HBED-CC PSMA-PET/CT: a planning study based on histopathology reference. Radiother Oncol 2017;123:472–7.

[2] Chang JH, Joon DL, Lee ST, Gong SJ, Anderson NJ, Scott AM, et al. Intensity modulated radiation therapy dose painting for localized prostate cancer using C-11-choline positron emission tomography scans. Int J Radiat Oncol 2012;83:E691–6.

[3] Pucar D, Hricak H, Shukla-Dave A, Kuroiwa K, Drobnjak M, Eastham J, et al. Clinically significant prostate cancer local recurrence after radiation therapy occurs at the site of primary tumor: magnetic resonance imaging and step-section pathology evidence. Int J Radiat Oncol 2007;69:62–9.

[4] Arrayeh E, Westphalen AC, Kurhanewicz J, Roach M, Jung AJ, Carroll PR, et al. Does local recurrence of prostate cancer after radiation therapy occur at the site of primary tumor? Results of a longitudinal MRI and MRSI study. Int J Radiat Oncol 2012;82:E787–93.

[5] Lips IM, van der Heide UA, Haustermans K, van Lin EN, Pos F, Franken SP, et al. Single blind randomized phase III trial to investigate the benefit of a focal lesion ablative microboost in prostate cancer (FLAME-trial): study protocol for a randomized controlled trial. Trials 2011;12:255.

[6] Bauman G, Haider M, Van der Heide UA, Menard C. Boosting imaging defined dominant prostatic tumors: a systematic review. Radiother Oncol 2013;107:274–81.

[7] Ruprecht O, Weisser P, Bodelle B, Ackermann H, Vogl TJ. MRI of the prostate: interobserver agreement compared with histopathologic outcome after radical prostatectomy. Eur J Radiol 2012;81:456–60.

[8] Steenbergen P, Haustermans K, Lerut E, Oyen R, De Weyer L, Van den Bergh L, et al. Prostate tumor delineation using multiparametric magnetic resonance imaging: inter-observer variability and pathology validation. Radiother Oncol 2015;115:186–90.

[9] van Schie MA, Dinh CV, Houdt PJV, Pos FJ, Heijmink S, Kerkmeijer LGW, et al. Contouring of prostate tumors on multiparametric MRI: evaluation of clinical delineations in a multicenter radiotherapy trial. Radiother Oncol 2018;128:321–6.

[10] Zamboglou C, Thomann B, Koubar K, Bronsert P, Krauss T, Rischke HC, et al. Focal dose escalation for prostate cancer using (68)Ga-HBED-CC PSMA PET/CT and MRI: a planning study based on histology reference. Radiat Oncol 2018;13:81.

[11] Zamboglou C, Drendel V, Jilg CA, Rischke HC, Beck TI, Schultze-Seemann W, et al. Comparison of 68Ga-HBED-CC PSMA-PET/CT and multiparametric MRI for gross tumour volume detection in patients with primary prostate cancer based on slice by slice comparison with histopathology. Theranostics 2017;7:228–37.

[12] Eiber M, Weirich G, Holzapfel K, Souvatzoglou M, Haller B, Rauscher I, et al. Simultaneous 68Ga-PSMA HBED-CC PET/MRI improves the localization of primary prostate cancer. Eur Urol 2016.

[13] Rhee H, Thomas P, Shepherd B, Greenslade S, Vela I, Russell PJ, et al. Prostate specific membrane antigen positron emission tomography may improve the diagnostic accuracy of multiparametric magnetic resonance imaging in

localized prostate cancer as confirmed by whole mount histopathology. J Urol 2016.
[14] Zamboglou C, Wieser G, Hennies S, Rempel I, Kirste S, Soschynski M, et al. MRI versus (68)Ga-PSMA PET/CT for gross tumour volume delineation in radiation treatment planning of primary prostate cancer. Eur J Nucl Med Mol Imaging 2016;43:889–97.
[15] Boellaard R, Hristova I, Ettinger S, Sera T, Stroobants S, Chiti A, et al. EARL FDG-PET/CT accreditation program: feasibility, overview and results of first 55 successfully accredited sites. J Nucl Med 2013;54:2052. Abstract (PW) Poster.
[16] Boellaard R, Hristova I, Ettinger S, Stroobants S, Chiti A, Bauer A, et al. Initial experience with the EANM accreditation procedure of FDG PET/CT devices. Eur J Cancer 2011;47:S8. Abstract (OP) Poster.
[17] Zamboglou C, Schiller F, Fechter T, Wieser G, Jilg CA, Chirindel A, et al. (68)Ga-HBED-CC-PSMA PET/CT versus histopathology in primary localized prostate cancer: a voxel-wise comparison. Theranostics 2016;6:1619–28.
[18] Bittner MI, Wiedenmann N, Bucher S, Hentschel M, Mix M, Rucker G, et al. Analysis of relation between hypoxia PET imaging and tissue-based biomarkers during head and neck radiochemotherapy. Acta Oncol 2016;55:1299–304.
[19] Oehlke O, Mix M, Graf E, Schimek-Jasch T, Nestle U, Gotz I, et al. Amino-acid PET versus MRI guided re-irradiation in patients with recurrent glioblastoma multiforme (GLIAA) – protocol of a randomized phase II trial (NOA 10/ARO 2013–1). BMC Cancer 2016;16.
[20] Benjamini Y, Krieger AM, Yekutieli D. Adaptive linear step-up procedures that control the false discovery rate. Biometrika 2006;93:491–507.
[21] Zou KH, Warfield SK, Bharatha A, Tempany CM, Kaus MR, Haker SJ, et al. Statistical validation of image segmentation quality based on a spatial overlap index. Acad Radiol 2004;11:178–89.
[22] Zschaeck S, Lohaus F, Beck M, Habl G, Kroeze S, Zamboglou C, et al. PSMA-PET based radiotherapy: a review of initial experiences, survey on current practice and future perspectives. Radiat Oncol 2018;13:90.
[23] Giesel FL, Sterzing F, Schlemmer HP, Holland-Letz T, Mier W, Rius M, et al. Intra-individual comparison of (68)Ga-PSMA-11-PET/CT and multi-parametric MR for imaging of primary prostate cancer. Eur J Nucl Med Mol Imaging 2016;43:1400–6.
[24] Thomas L, Kantz S, Hung A, Monaco D, Gaertner FC, Essler M, et al. (68)Ga-PSMA-PET/CT imaging of localized primary prostate cancer patients for intensity modulated radiation therapy treatment planning with integrated boost. Eur J Nucl Med Mol Imaging 2018;45:1170–8.
[25] Rischke HC, Nestle U, Fechter T, Doll C, Volegova-Neher N, Henne K, et al. 3 Tesla multiparametric MRI for GTV-definition of dominant intraprostatic lesions in patients with prostate cancer–an interobserver variability study. Radiat Oncol 2013;8:183.
[26] Bravaccini S, Puccetti M, Bocchini M, Ravaioli S, Celli M, Scarpi E, et al. PSMA expression: a potential ally for the pathologist in prostate cancer diagnosis. Sci Rep 2018;8:4254.
[27] Su F, Zhang W, Zhang D, Zhang Y, Pang C, Huang Y, et al. Spatial intratumor genomic heterogeneity within localized prostate cancer revealed by single-nucleus sequencing. Eur Urol 2018;74:551–9.
[28] Mannweiler S, Amersdorfer P, Trajanoski S, Terrett JA, King D, Mehes G. Heterogeneity of prostate-specific membrane antigen (PSMA) expression in prostate carcinoma with distant metastasis. Pathol Oncol Res 2009;15:167–72.